 doi:10.20944/preprints201812.0124.v1

Highly sensitive formaldehyde detection using well-aligned zinc oxide nanosheets synthesized by Chemical Bath Deposition technique

Eun-Bi Kim, Hyung-Kee Seo*

School of Chemical Engineering, Chonbuk National University, Jeonju 54896, Republic of Korea

Abstract

Detection of formaldehyde is very important in terms of life protection, as it can cause serious injury to eyes, skin, mouth and gastrointestinal function if indirectly inhaled and hence researchers are putting effort in developing novel and sensitive device. In this work, we have fabricated an electro-chemical sensor in the form of a field effect transistor (FET) to detect formaldehyde over wide range (10 nM to 1mM). For this, ZnO nanosheets (NS) were first synthesized by hydrothermal method with in-situ deposition on cleaned SiO_2 coated Si (100) substrate. The synthesized materials were characterized for morphology and purity and surface area (31.718 m^2/g). The developed device was tested for formaldehyde detection at room temperature that resulted in a linear response with concentration (96%), sensitivity value of 0.27 $mA/M/cm^2$ and a low detection limit of 210 nM, and a high 0.93194 return.

Keyword: ZnO, Nanosheet, Formaldehyde, Chemical sensor, FET

*Corresponding authors. Fax: +82 63 270 2306
E-mail addresses: hkseo@jbnu.ac.kr

Preprints (www.preprints.org) | NOT PEER-REVIEWED | Posted: 11 December 2018 doi:10.20944/preprints201812.0124.v1

Introduction

Among the metal oxides, ZnO, SnO_2, TiO_2, Fe_2O_3, and WO_3 are attractive materials due to their unique properties such as high electron mobility, fast electron transfer rate, material stability etc. One of them; ZnO; has been widely used in many optoelectronic and sensing devices owing to its optical/electrical properties. Zinc oxide nanomaterial-based electrodes also exhibit excellent electrochemical activity against chemicals, biomolecules and gases due to their high electron transfer characteristics and photochemical stability [1-8].

Detection of formaldehyde is very important in terms of life protection, as it can cause serious injury to eyes, skin, mouth and gastrointestinal function if indirectly inhaled. [9-12].

Xinxin Xing et al. used convenient solution combustion method for the synthesis of Ag-loaded ZnO and reported as hierarchically porous heterojunction nanocomposites and varied the Ag contents and used it for the detection of formaldehyde in gaseous form at 240°C[13]. Shaohong Wei et al. synthesized hollow nanofibers of SnO_2–ZnO, for formaldehyde detection sensing properties and reported optimum performance at 260°C down to 0.1 ppm with good selectivity and stability, rapid response–recovery time and high sensitivity [14]. In another report, Zi-Wei Chen et al. used pure ZnO and graphene doped ZnO with different morphologies synthesized by hydrothermal process at 150 °C for formaldehyde gas sensing performance, in the range of 2 to 2000 ppm, and reported to deliver good selectivity and fast response/recovery time and at 200 °C [15]. Linqi Shi et al. used ZnO architectures in a three dimensional (3D) center-hollow form and studied to photoelectric gas-sensing that exhibited good selectivity to formaldehyde and excellent sensitivity at 365 nm light irradiation by conducting the measurement at room temperature. Po-Ren Chung et al. published a review on formaldehyde gas sensing with sufficient literature survey and mentions that many methods based on spectrophotometric, fluorometric, piezoresistive, amperometric or conductive measurements have been proposed for detecting the concentration of formaldehyde in air. However, conventional formaldehyde measurement systems are bulky and expensive and require the services of highly-trained operators [16]. This has inspired us to explore the possibility of an electrochemical detection of formaldehyde in the form of a FET device that can deliver better performance at room temperature.

Preprints (www.preprints.org) | NOT PEER-REVIEWED | Posted: 11 December 2018 doi:10.20944/preprints201812.0124.v1

In this work, we synthesized zinc oxide nanostructures using a simple hydrothermal method and fabricated a chemical sensor that detects formaldehyde. For sensor fabrication, synthesized nanostructures were deposited on a Si/SiO_2 substrate using CBD that resulted into a uniformly aligned nanosheet electrodes. The electrochemical sensor was fabricated in the form of a FET device and the electrochemical characteristics were determined with various concentrations of formaldehyde (10 nM~1 mM in 0.1 M) in phosphate buffer (PBS) to determine the sensing properties.

2. Experimental details

2.1 ZnO NS synthesis

In this work, ZnO NS was synthesized by hydrothermal synthesis using zinc nitrate hexahydrate ($Zn(NO_3)_2 \cdot 6H_2O$, ≥ 99.0%, Sigma Aldrich) and Urea (NH_2CONH_2, ≥ 99%, Sigma Aldrich). In a typical reaction, 0.02 M zinc nitrate hexahydrate and ~16.67% urea was dissolved in 100 mL of distilled water and stirred well for 30 min. This solution was used for synthesis of ZnO which was loaded in the Teflon coated vessel of hydrothermal reactor. In order to deposit films of ZnO during hydrothermal synthesis, the pre-coated Si/SiO_2 substrate were dipped in the solution and vessel was sealed.

Before loading the substrate into the hydrothermal reactor, cleaned substrates were coated with a thin layer of silver through thermal evaporator that can be used as one of the electrodes of FET. The hydrothermal reaction was then carried out at 80°C for 5 hours. After cooling the reactor to room temperature, the substrates were removed and thoroughly washed with distilled water, ethanol and acetone to remove impurities and unreacted reactants. The substrate on which ZnO NS was deposited was dried in an oven at 60 °C for 12 hours and then sintered at 200 °C for 2 hours.

2.2 Material characterization

The synthesized ZnO NS were characterized for morphology by Field Emission Scanning Electron Microscopy (FESEM, Hitachi S-4700), and Transmission Electron Microscopy (TEM, JEM-ARM200F). Elemental analysis was done by Energy Dispersive Spectroscopy (EDS, Hitachi), X-ray diffractometer (XRD, Ultima IV, Rigaku) and Fourier Transform Infrared Spectroscopy (FTIR, Nicolet, IR300) other than analyzing the crystallinity and component properties. The optical properties

Preprints (www.preprints.org) | NOT PEER-REVIEWED | Posted: 11 December 2018 doi:10.20944/preprints201812.0124.v1

were studied by obtaining Ultraviolet-visible spectra (UV-vis, JASCO, V-670). Specific surface area analysis was performed to investigate the specific surface area of nanostructures by BET Technique (Micromeritics, ASAP 2010).

2.3 ZnO NS FET sensor fabrication and Detection of Formaldehyde

For the fabrication of ZnO NS FET-sensor, p-type Si wafer with (100) orientation was cleaned by acetone, ethanol, and DI water, followed by drying with nitrogen (N_2) gas. The source and drain gold (Au) electrode was deposited to a thickness of ~100−150 nm by thermal evaporation mounted with thickness monitor. After electrodes, the slurry of Zn NS powder was made with 30 wt% polyethylene glycol (PEG 20000, pure, JUNSEI) as binder and the film was deposited through the screen printing followed by annealing at ~400 °C for 1 h. Zn NS was applied as channeling materials in between source and drain of the FET. In last step, the deposited Zn NS over Au-Si/SiO_2 based FET was used for the detection of formaldehyde using the reported method [17].

For electrochemical detection experiments to be performed, various concentrations of formaldehyde was prepared in the range of 10 nM~1 mM in phosphate buffer solution (PBS, 0.1 M) with Ag / AgCl electrode as a counter electrode. The gate voltage (V_G) was varied from 0 to 2V and the resulting drain current (I_D) value was recorded. The sensitivity was then calculated through the drain current value.

3. Result and discussion

FE-SEM was used to analyze surface morphology and size of ZnO NS, which also gave an idea about the uniform coating of the screen printed film of ZnO. The micrographs in Fig. 1 indicates that the ZnO NS are of sheet like structure and uniformly deposited on the substrate (Fig. 1a and 1b, low magnification images). The thickness estimated from the image is ~ 6 to 8 μm. The insets shows the larger area view where the uniform layer and thickness is seen. Fig. 1 (c) shows the high resolution image and the element mapping (inset) obtained with EDS to investigate the composition of ZnO NS, where Zn and O elements are seen uniformly distributed and no other impurities/elements are noticed. The ZnO NS was also observed by using transmission electron microscope (TEM), high resolution

 doi:10.20944/preprints201812.0124.v1

transmission electron microscope (HR-TEM) and selected area diffraction pattern (SAED). Low-magnification TEM image of a ZnO NS (Fig. 1 d) shows that a uniform lattice without any disorders indicating pure material quality. Further, high-resolution TEM, SAED and Fast Fourier Transform (FFT) was used to confirm the lattice characteristics, which shows that the lattice grew at 0.27 nm intervals on the (011) plane.

To investigate the specific surface area of hydrothermally synthesized ZnO NS, a specific surface area analysis was carried out, that was measured by using physical adsorption and chemical adsorption of nitrogen gas which showed a specific surface area of 31.718 m^2 / g, which is fairly large specific surface area as compared with zinc oxide of other nanostructures [18-19]. It is well know that nanostructures with larger specific surface area would have greater sensitivity owing to large surface area available for interaction/adsorption [20].

Fourier transform infrared spectroscopic spectrum (FTIR, Fig. 2a) shows a strong IR band at 557 cm^{-1}, indicating the bonding of Zn-O, which is a metal oxide. It corresponds to the scissile vibration of water molecules and the stretching mode of O-H at 1633 cm^{-1} and 3452 cm^{-1}, respectively. The FTIR results showed that the synthesized material is of high purity analogous to the HRTEM results. Phase and crystallinity of ZnO NS was confirmed by obtaining X-ray diffraction pattern (XRD, Rigaku, CuKa, λ = 1.54178 Å) which is shown in Fig. 2 (b). The diffraction peaks are observed at the Bragg angle of 31.73º (010), 34.329º (002), 36.19º (011), 47.44º (012), 56.52º (110), 62.70º (013), 66.28º (020), 67.382º (112), 68.98º (021), 72.35º (004), and 76.82º (014). Our ZnO Wurzite structure data is well agreement with the Joint Committee on Powder Diffraction Standard (JCPDS) card no JCPDS PDF no 36-1451 [21]. Diffraction peaks other than the main peak of ZnO were not detected, which again confirmed a pure ZnO. It was found that the synthesized ZnO NS had a good crystallinity and mainly a (011) plane orientation. Fig. 2c shows the absorbance spectra of the synthesized material acquired ultraviolet spectroscopy (UV-vis). It is seen that the peak absorption is at 362 nm. The optical band gap, as calculated from the absorption spectrum, is ~ 3.4 eV, which is the known optical band gap of the ZnO nanomaterial. Fig. 2d shows the Photo Luminescence spectrum of ZnO NS obtained at room temperature, where the absorption peak is observed at 371 nm.

Preprints (www.preprints.org) | NOT PEER-REVIEWED | Posted: 11 December 2018 doi:10.20944/preprints201812.0124.v1

Sensing Characteristics

A field effect transistor (FET) device was fabricated to develop and electrochemical sensing device for formaldehyde using ZnO NS as channel material (1 cm^2) for drain and source and silver a gate electrode. The electrode configuration used for sensing is shown in fig. 3 (a). The gate voltage (V_G) was varied from 0 to 2V and the resulting drain current (I_D) value was recorded. The device parameters such sensitivity, minimum detection limit and regression coefficient were then calculated through the drain current value. A typical drain current (V_{SG}-I_D) curve as a function of gate voltage with and without formaldehyde is show in Fig. 3 (b) which shows a remarkable difference in the current response as magnitude of current without the formaldehyde is low, while the current observed after addition of the formaldehyde (10 nM) is higher. The data clearly shows the potential sensing characteristic of the synthesized material. Inspired with this observation, the I-V curve were then obtained with varying concentrations of formaldehyde (10nM, 100 nM, 1µM, 10 µM, 100 µM and 1 mM in 0.1 M PBS) which are shown in Fig. 3c. It can be seen that the current increases with the increasing concentration amount due to increased electron movement resulting out of the reduction of ZnO NS with formaldehyde. At the same time the current values of each curve have changed with concentration that can be used a measure of the indirect sensitivity value of the device for formaldehyde detection. To estimate the sensitivity, the drain current value at the gate voltage of 1.5V was plotted with concentration, which is shown as Fig. 3d. It can be seen that the developed device is able to deliver a linear response to formaldehyde concentration to an extent of 96% (regression coefficient). This curve was used to determine the sensitivity which is estimated ~ 0.27 mA/M/cm^2 and the estimated detection limit is 210 nM.

4. Conclusion

Zinc oxide nanosheet like structure was directly grown on pre-cleaned Si (100) substrate by hydrothermal synthesis at 180°C. The synthesized materials structure was confirmed with FESEM and TEM observations while purity was confirmed with FTIR and HRTEM. With nanosheet like structure, we were able to get a specific surface area of ~31.718 m^2/g that delivered good sensitivity for formaldehyde in the form of a FET device at room temperature. The detection sensitivity of the formaldehyde is found as 0.27 mA/M/cm^2 and the device is offering a detection limit up to 210 nM

 doi:10.20944/preprints201812.0124.v1

which is a fairly low value indicating the possibility of using the developed FET as a commercial detection device.

Acknowledgments

"This research was supported by Basic Science Research program through the National Research Foundation of Korea (NRF) funded by the Ministry of Education (#1701002686). "This paper was supported by research funds for newly appointed professors of Chonbuk National University in 2015"

 doi:10.20944/preprints201812.0124.v1

References

[1 Xu S.; Wang Z.L. One-dimensional ZnO nanostructures: Solution growth and functional properties, *Nano Res.* **2011**, *4*, 1013-1098.

[2] Fan Z.; Lu J.G. Zinc Oxide Nanostructures: Synthesis and Properties, *J. NanoSci. Nanotech.* **2005**, *5*, 1561-1573.

[3] Kalandaragh Y.A.; Khodayari A.; Behboudni M. Ultrasound-assisted synthesis of ZnO semiconductor nanostructures, *Mater. Sci. Semicon. Proc.* **2009**, *12*, 142-145.

[4] Zang Z.; Zeng X.; Du J.; Wang M.; Tang X. Femtosecond laser direct writing of microholes on roughened ZnO for output power enhancement of InGaN light-emitting diodes, *Optics Lett*. **2016**, *41*, 3463-3466.

[5] Zang Z.; Tang X. Enhanced fluorescence imaging performance of hydrophobic colloidal ZnO nanoparticles by a facile method, *J. Alloys Compd.* **2015**, *619*, 98-101.

[6] Rosli N.I.M.; Lam S.M.; Sin J.C.; Mohamed A.R. Surfactant-free precipitation synthesis, growth mechanism and photocatalytic studies of ZnO nanostructures, *Mater. Lett*. **2015**, *160*, 259-262.

[7] Mansouri S.; Khalili S.; Jahanshahi M.; Darabi R.R.; Ardeshiri F.; Rad A.S.; Sublayer assisted by hydrophilic and hydrophobic ZnO nanoparticles toward engineered osmosis process, *Korean. J. Chem. Eng*. **2018**, *35*, 2256-2268.

[8] Straumal B.B.; Protasova S.G.; Mazilkin A.A.; Straumal P.B.; Schütz G.; Tietze T.; Goering E.; Baretzky B. Ferromagnetic behaviour of Fe-doped ZnO nanograined films, *Beilstein J. Nanotechnol*. **2013**, *4*, 361-369.

[9] Wei W.; Guo S.; Chen C.; Sun L.; Chen Y.; Guo W.; Ruan S. High sensitive and fast formaldehyde gas sensor based on Ag-doped LaFeO3 nanofibers, *J. Alloys and Comp*. **2017,** *695*, 1122-1127.

[10] Sakai K.; Norbäck D.; Mi Y.; Shibata E.; Kamijima M.; Yamada T.; Takeuchi Y. A comparison of indoor air pollutants in Japan and Sweden: formaldehyde, nitrogen dioxide, and chlorinated volatile organic compounds, *Environ. Res*. **2004**, *94*, 75-85.

[11] Feng L.; Liu Y.; Zhou X.; Hu J. The fabrication and characterization of a formaldehyde odor sensor using molecularly imprinted polymers, *J. Colloid Interface Sci*. **2005**, *284*, 378-382.

[12] Kim K.H.; Jahan S.A.; Lee J.T. Exposure to formaldehyde and its potential human health Hazards, *J. Environ. Sci. Health Part C*, **2011**, *29*, 277-299.

[13] Xing X.; Xiao X.; Wang L.; Wang Y. Highly sensitive formaldehyde gas sensor based on hierarchically porous Ag-loaded ZnO heterojunction nanocomposites, *Sens. Actuators B: Chem.* **2017**, *247*, 797-806.

[14] Wei S.; Zhang Y.; Zhou M. Formaldehyde sensing properties of ZnO-based hollow nanofibers, *Sensor Rev.* **2014**, *3*, 327-334.

[15] Chen Z.W.; Hong Y.Y.; Lin Z.D.; Liu L.M.; Zhang X.W. Enhanced formaldehyde gas sensing properties of ZnO nanosheets modified with graphene, *Electron. Mater. Lett.* **2017**, *13*, 270-276.

[16] Chung P.R.; Tzeng C.T.; Ke M.T.; Lee C.Y. Formaldehyde Gas Sensors: A Review, *Sens.* **2013**, *13*, 4468-4484.

[17] Kim E.B.; Ameen S.; Akhtar M.S.; Shin H-S. Iron-nickel co-doped ZnO nanoparticles as scaffold for field effect transistor sensor: Application in electrochemical detection of hexahydropyridine chemical, *Sens. Actuators B.Chem.* **2018**, *275*, 422-431.

[18] Thirumavalavan M.; Huang K.L.; Lee J.F. Preparation and Morphology Studies of Nano Zinc Oxide Obtained Using Native and Modified Chitosans, *Mater.* **2013**, *6*, 4198-4212.

[19] Liang Y.; Guo N.; Li L.; Li R.; Ji G.; Gan S. Preparation of porous 3D Ce-doped ZnO microflowers with enhanced photocatalytic performance, *RSC Adv.* **2015**, *5*, 59887-59894.

[20] Kim J.Y.; Jo S.Y.; Sun G.J.; Katoch A.; Choi S.W.; Kim S. S. Tailoring the surface area of ZnO nanorods for improved performance in glucose sensors, *Sens. Actuators B.Chem.* **2014**, *192*, 216-220.

[21] Aim K.A.; Fonoberov V.A.; Shamsa M.; Balandin A.A. Micro-Raman investigation of optical phonons in ZnO nanocrystals, *J. Appl. Phys.* **2005**, *97*, 124313-1~5.

 doi:10.20944/preprints201812.0124.v1

Figure list

Table list

 doi:10.20944/preprints201812.0124.v1

Fig. 1

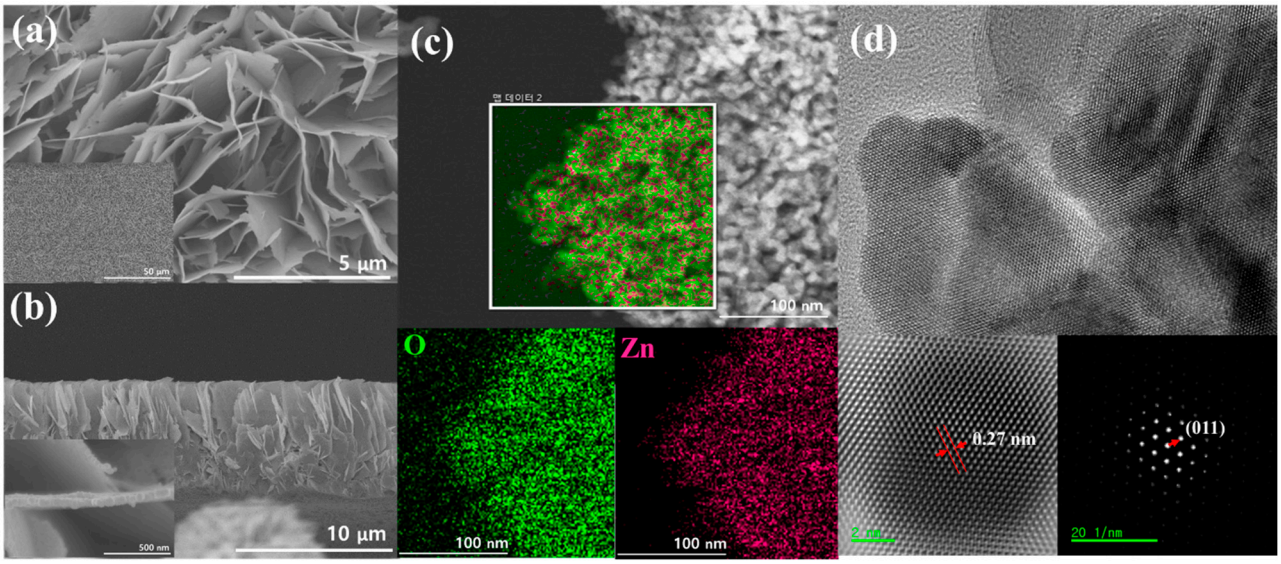

Preprints (www.preprints.org) | NOT PEER-REVIEWED | Posted: 11 December 2018 doi:10.20944/preprints201812.0124.v1

Fig. 2

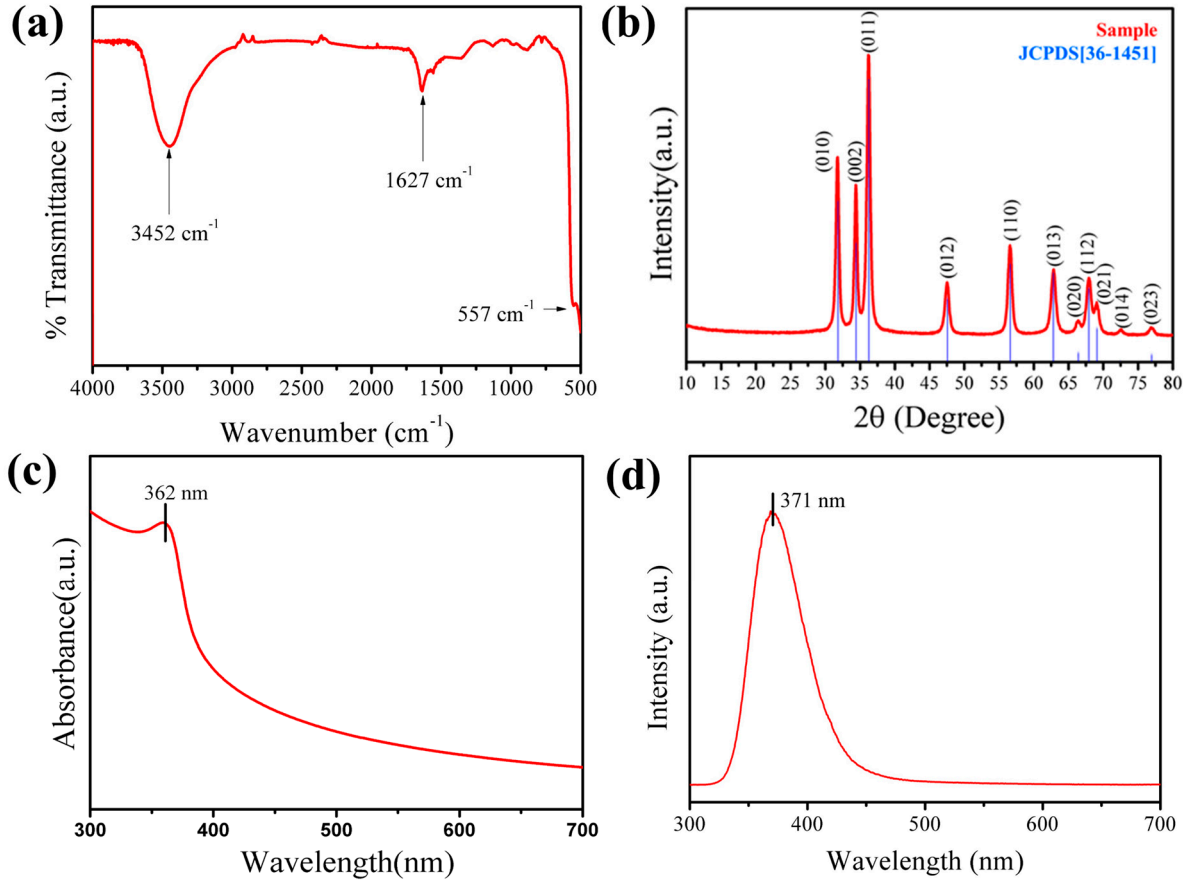

Preprints (www.preprints.org) | NOT PEER-REVIEWED | Posted: 11 December 2018 doi:10.20944/preprints201812.0124.v1

Fig. 3

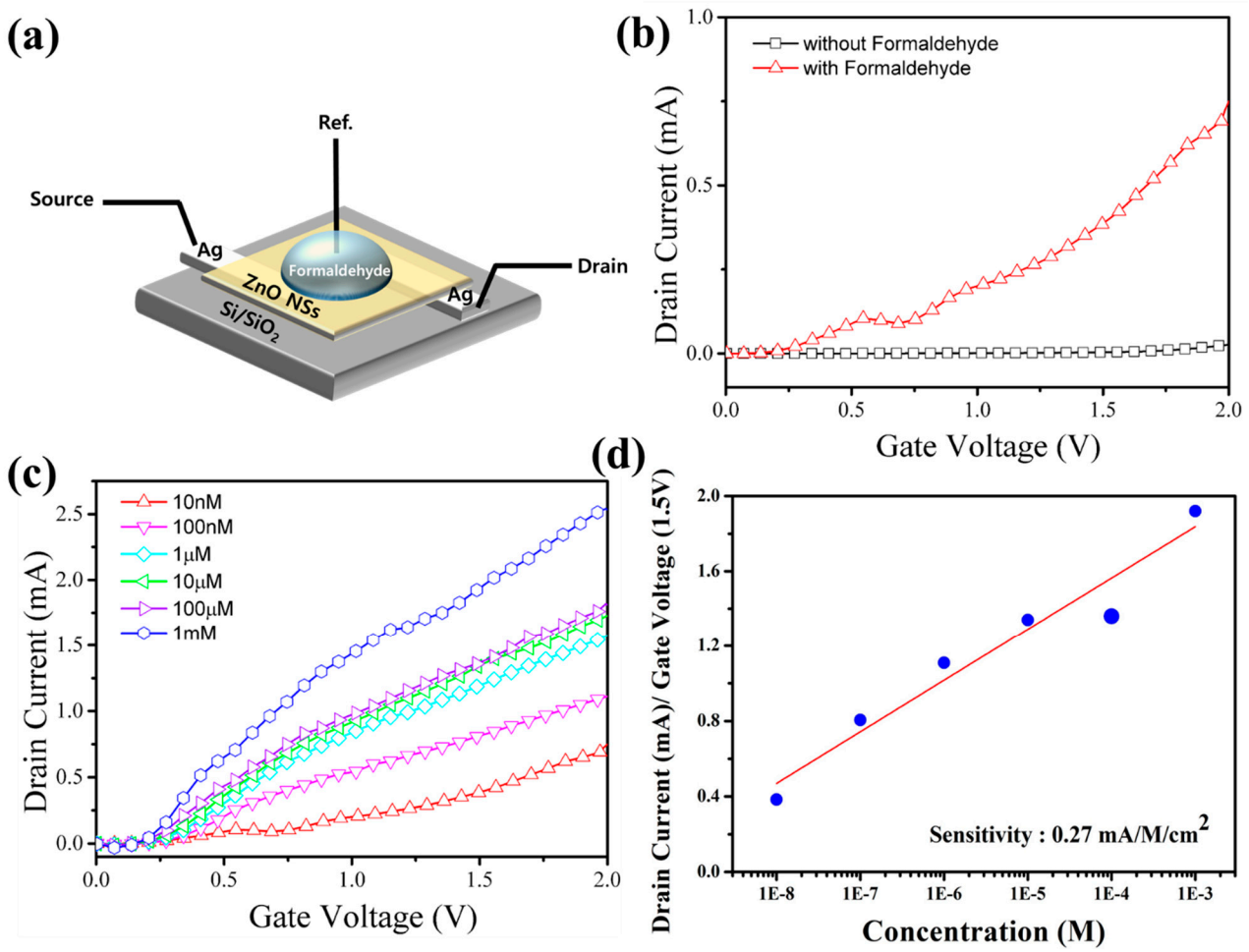

Preprints (www.preprints.org) | NOT PEER-REVIEWED | Posted: 11 December 2018 doi:10.20944/preprints201812.0124.v1

Table 1.

Sample	BET Surface Area (m^2/g)	Average pore diameter (nm)	Reference
ZnO particle	2.3485	8.96	[18]
ZnO microflower	10.47	18.62	[19]
ZnO NSs	31.718	33.982	[present]